Digital Commons @ LMU and LLS

**Digital Commons@
Loyola Marymount University
and Loyola Law School**

Electrical Engineering & Computer Science Faculty Works

Electrical Engineering & Computer Science

Improving the Performance of Single Chip Image Capture Devices

Barbara E. Marino
Loyola Marymount University, bmarino@lmu.edu

Robert L. Stevenson
University of Notre Dame

Improving the performance of single chip image capture devices

Barbara E. Marino
Loyola Marymount University
Department of Electrical Engineering and Computer Science
Los Angeles, California 90045
E-mail: bmarino@lmu.edu

Robert L. Stevenson
University of Notre Dame
Laboratory for Image and Signal Analysis
Department of Electrical Engineering
Notre Dame, Indiana 46556

Abstract. *Single chip charge-coupled devices (CCDs) coupled with filters for isolating red, green, and blue color content are commonly used to capture color images. While this is more cost effective than multiple chip systems, best results are obtained when full RGB color information is obtained for every point in an image. The process of color subsampling in a single chip system degrades the resulting image data by introducing artifacts such as blurry edges and false coloring. We propose an algorithm for enhancing color image data that were captured with a typical single chip CCD array. The algorithm is based on stochastic regularization using a Markov random field model for the image data. This results in a constrained optimization problem, which is solved using an iterative constrained gradient descent computational algorithm. Results of the proposed algorithm show a marked improvement over the original sampled image data.* © 2003 SPIE and IS&T. [DOI: 10.1117/1.1560643]

1 Introduction

The capture of color image information for digital processing requires the measurement of at least three color spectral bands at all points of the image using a color scanner or camera. Typically, color is measured using a combination of filters and light-sensitive elements, such as charge-coupled devices (CCDs), to measure the red, green, and blue content of the image. Optimally this is done by alternately isolating each color primary and measuring the intensity of each color at each point in the image. This is done using either a single CCD array with multiple exposures through different color filters or by using multiple CCD arrays with different color filters. Since multiple CCD systems are expensive and multiple exposures are often not practical, single chip CCD systems have been developed. Individual elements of the CCD array are each coupled with a filter for measuring the color content of one of the primaries. These individual filters are arranged in a mosaic

pattern over the array, which effectively samples the image data since each element in the CCD array can only measure one color.

Since the different spectral bands are no longer being sampled at the same physical location, color artifacts are often introduced. These artifacts are most noticeable at edge locations where the edges in each of the color primaries do not correlate with each other. This introduces blurry edges and false coloring. The artifacts can be greatly improved by processing the image after it has been captured.[1]

Researchers have proposed a wide variety of methods to reduce these artifacts. Ozawa and Takahashi,[2,3] and Sugiura, Asakawa, and Fujino[4] examined this problem as it pertains to digital video cameras. Omori and Ueda[5] determined a corrected, high-resolution image using multiple images of the same object, shifted in phase. Messing and Sezan[6] used multiple images captured by a camera operating in burst mode to produce a single high resolution image.

This problem as it pertains to digital still cameras has been examined from many different perspectives. Go, Sohn, and Lee[7] investigated an interpolation scheme based on neural networks. Sakamoto, Nakanishi, and Hase,[8] and Toi[9] explored algorithms as suitable and optimal for specific platforms.

One prominant artifact produced from single chip image capture is the false coloring introduced when the edges of objects appear misaligned in different spectral bands. To compensate for this, researchers have proposed algorithms that employ cross-channel correlation. This research includes the work of Hur and Kang,[10] Kimmel,[11] and Kuno and Sugiura.[12] These methods are simple, noniterative weighted interpolation schemes.

We propose an interative algorithm for improving the results of single chip color image capture. The algorithm is based on stochastic regularization using a Gaussian image model with a deterministic line process to realign the edge information. The image model is used in a maximum *a*

Fig. 1 Single chip CCD array.

Fig. 2 Subsampling.

$$\mathbf{Y}_{i,j} = \begin{bmatrix} r \\ g \\ b \end{bmatrix}_{i,j}, \qquad (1)$$

posteriori estimation technique, resulting in a constrained optimization problem. This is optimized using an iterative constrained gradient descent computational algorithm.

Section 2 describes the forward process of capturing an image using a single chip CCD array. The estimation technique and the proposed algorithm used in the enhancement process are introduced in Sec. 3. Section 4 presents the results of testing the proposed algorithm, and Sec. 5 summarizes the results of this work.

2 Color Image Capture Using a Single Chip CCD Array

As mentioned in the previous section, color image data can be measured using a single chip CCD array. The layout of a typical single chip CCD array is shown in Fig. 1.[13] The letters R, G, and B represent the filter associated with each particular CCD element given its spatial location in the array. An element labeled *R* is coupled with a filter that enables the element to isolate and measure the red content of the image at that particular location. Similarly, G elements measure green information and B elements measure blue information.

Notice that there are as many green elements as red and blue combined. Single chip color CCDs are designed this way, since green appears brighter to the human visual system (HVS) than other colors.[14] Green therefore carries more visually important information than red or blue. During the image capture process, the values measured by the two green elements in the same 2×2 block are averaged to produce a single value of green.

Measuring color information in this way effectively subsamples the color data by a factor of 2 in each dimension, resulting in one value of each of the color primaries for each 2×2 block of pixels in the original image. A more traditional technique for subsampling is accomplished by averaging the values of each color primary in the block. For the purpose of this discussion we refer to this traditional means of subsampling as proper subsampling.

Let **X** represent a full resolution $M \times N$ color image in RGB space, where $\mathbf{X} \in \mathcal{V}^{MN}$, $\mathcal{V} = [0,1]$.[3] Let **Y** represent the results of properly subsampling **X** by a factor of 2 in each direction, $\mathbf{Y} \in \mathcal{V}^{MN/4}$. A color pixel at the (i, j) pixel location of the subsampled image **Y** is denoted by a vector in 3-D space, $\mathbf{Y}_{i,j}$, where r, g, and b are the color elements of that vector. That is,

where r, g, $b \in [0,1]$.

For notational convenience a pixel in the full resolution image $\mathbf{X}_{i,j}$ is defined to contain the pixel values of the 2×2 sampling block of a CCD array, see Fig. 2. In this case the vector $\mathbf{X}_{i,j}$ contains four elements for each of the primaries,

$$\mathbf{X}_{i,j} = [R_{0,0}\ R_{0,1}\ R_{1,0}\ R_{1,1}\ G_{0,0}\ G_{0,1}\ G_{1,0}\ G_{1,1}\ B_{0,0}\ B_{0,1}\ B_{1,0}\ B_{1,1}]^t_{i,j}, \qquad (2)$$

where the values of the elements of this vector are also contained in the interval $[0, 1]$.

The forward process of obtaining a properly subsampled image **Y** from a full resolution image **X** is given by,

$$\mathbf{Y}_{i,j} = \begin{bmatrix} \frac{1}{4} & \frac{1}{4} & \frac{1}{4} & \frac{1}{4} & 0 & 0 & 0 & 0 & 0 & 0 & 0 & 0 \\ 0 & 0 & 0 & 0 & \frac{1}{4} & \frac{1}{4} & \frac{1}{4} & \frac{1}{4} & 0 & 0 & 0 & 0 \\ 0 & 0 & 0 & 0 & 0 & 0 & 0 & 0 & \frac{1}{4} & \frac{1}{4} & \frac{1}{4} & \frac{1}{4} \end{bmatrix} \mathbf{X}_{i,j} = \mathbf{S} \mathbf{X}_{i,j}. \qquad (3)$$

A matrix $\underline{\mathbf{S}}$, which subsamples the complete original image,

$$\mathbf{Y} = \underline{\mathbf{S}} \mathbf{X}, \qquad (4)$$

can be appropriately formed from the template matrices **S**.

Improper subsampling achieved by capturing an image using a single chip CCD array is given by the equation

$$\mathbf{Y}^*_{i,j}$$

$$= \begin{bmatrix} 1 & 0 & 0 & 0 & 0 & 0 & 0 & 0 & 0 & 0 & 0 & 0 \\ 0 & 0 & 0 & 0 & 0 & \frac{1}{2} & \frac{1}{2} & 0 & 0 & 0 & 0 & 0 \\ 0 & 0 & 0 & 0 & 0 & 0 & 0 & 0 & 0 & 0 & 0 & 1 \end{bmatrix} \mathbf{X}_{i,j} = \mathbf{S}^* \mathbf{X}_{i,j}. \qquad (5)$$

Again, a matrix can be appropriately formed to describe the process of improperly subsampling the complete image,

$$\mathbf{Y}^* = \underline{\mathbf{S}}^* \mathbf{X}, \qquad (6)$$

where $\mathbf{Y}^*$ represents the results of improperly subsampling **X**.

3 Bayesian Estimation and the Enhancement Process

The enhancement process involves estimating $\mathbf{Y}$ from $\mathbf{Y}^*$. Let the estimate of the properly sampled color image data be represented by $\hat{\mathbf{Y}}$. This estimation problem is ill posed, since there is no unique solution. One method of estimating a unique, and thus well-posed solution is through Bayesian estimation.

To determine the estimate $\hat{\mathbf{Y}}$ of the properly sampled color image data $\mathbf{Y}$, from the improperly sampled data $\mathbf{Y}^*$, a maximum *a posteriori* (MAP) technique is used. Employing this technique, the estimate $\hat{\mathbf{Y}}$ can be written

$$\hat{\mathbf{Y}} = \arg \max_{\mathbf{Y} \in \mathcal{V}^{MN/4}} \log \Pr(\mathbf{Y}|\mathbf{Y}^*). \tag{7}$$

Using Bayes rule,

$$
\begin{aligned}
\Pr(\mathbf{Y}|\mathbf{Y}^*) &= \frac{\Pr(\mathbf{Y}^*|\mathbf{Y})\Pr(\mathbf{Y})}{\Pr(\mathbf{Y}^*)} \\
&= \frac{\Pr(\mathbf{Y}^*|\mathbf{X})\Pr(\mathbf{X}|\mathbf{Y})\Pr(\mathbf{Y})}{\Pr(\mathbf{Y}^*)} \\
&= \frac{\Pr(\mathbf{Y}^*|\mathbf{X})\Pr(\mathbf{Y}|\mathbf{X})\Pr(\mathbf{X})}{\Pr(\mathbf{Y}^*)},
\end{aligned}
\tag{8}
$$

which gives the estimation the form,

$$
\begin{aligned}
\hat{\mathbf{Y}} = \arg \min_{\mathbf{Y} \in \mathcal{V}^{MN/4}} \{ &-\log \Pr(\mathbf{Y}|\mathbf{X}) - \log \Pr(\mathbf{Y}^*|\mathbf{X}) \\
&-\log \Pr(\mathbf{X}) \}.
\end{aligned}
\tag{9}
$$

The full resolution image $\mathbf{X}$ is introduced into the estimation problem, since we have a good model for $\Pr(\mathbf{X})$. The conditional densities are based on our knowledge of the subsampled image given the original image data. Since the sampling process is known for both the proper and improper cases, these conditional densities are known exactly,

$$\Pr(\mathbf{Y}|\mathbf{X}) = \begin{cases} 0, & \mathbf{Y} \neq \underline{\mathbf{S}}(\mathbf{X}) \\ 1, & \mathbf{Y} = \underline{\mathbf{S}}(\mathbf{X}) \end{cases}, \tag{10}$$

$$\Pr(\mathbf{Y}^*|\mathbf{X}) = \begin{cases} 0, & \mathbf{Y}^* \neq \underline{\mathbf{S}}^*\mathbf{X} \\ 1, & \mathbf{Y}^* = \underline{\mathbf{S}}^*\mathbf{X} \end{cases}. \tag{11}$$

To model the image data, a Markov random field (MRF) is assumed with the Gibbs density function

$$\Pr(\mathbf{X}) = \frac{1}{Z} \exp\left[-\frac{1}{\lambda} \sum_{c \in C} \rho(\mathbf{d}_c^t \mathbf{X}) \right], \tag{12}$$

where Z is a normalizing constant, λ is the regularizing parameter, c is a local group of pixels called cliques, C is the set of all cliques throughout the image, $\mathbf{d}_c$ is a coefficient vector for clique c, and $\rho(\cdot)$ is a function of the cliques, which is further defined later.

A MAP estimate for this estimation problem can be found by solving the following minimization problem:

$$\hat{\mathbf{Y}} = \underline{\mathbf{S}}\left[\arg \min_{\mathbf{X} \in \mathcal{Z}} \left\{ \sum_{c \in C} \rho(\mathbf{d}_c^t \mathbf{X}) \right\} \right], \tag{13}$$

where $\mathcal{Z}$ is defined as the set of all possible images that solve the forward problem, i.e.,

$$\mathcal{Z} = \{ \mathbf{X} \in \mathcal{V}^{MN} : \mathbf{Y}^* = \underline{\mathbf{S}}^* \mathbf{X} \}. \tag{14}$$

Let

$$\hat{\mathbf{X}} = \arg \min_{\mathbf{X} \in \mathcal{Z}} \left\{ \sum_{c \in C} \rho(\mathbf{d}_c^t \mathbf{X}) \right\}. \tag{15}$$

From Eq. (13) we see that $\hat{\mathbf{X}}$ can first be computed and then used to determine $\hat{\mathbf{Y}}$ as follows,

$$\hat{\mathbf{Y}} = \underline{\mathbf{S}}\hat{\mathbf{X}}. \tag{16}$$

The derivation of this minimization problem has been sparse. It is desired only to summarize well-known results. For further information, the reader is referred to Refs. 15 and 16.

The quality of the resulting estimate of $\hat{\mathbf{X}}$ depends on the form of $\rho(\cdot)$ and $\mathbf{d}_c$. The function $\rho(\cdot)$ and the coefficients in $\mathbf{d}_c$ are set based on *a priori* assumptions about the image data. The *a priori* assumption that is incorporated into this work is that image data are basically smooth, however, edge information must be maintained and realigned.

For the first part of the assumption, the coefficients in $\mathbf{d}_c$ are set so that $\mathbf{d}_c^t \mathbf{X}$ provides a measure of smoothness. This is done by using finite difference approximations to a first-order derivative as the image data smoothness measure. At pixel $X_{i,j}$ the four discrete directional derivatives approximate a rotationally symmetric operator within a 3×3 pixel grid and are given as

$$\mathbf{d}_{i,j,0}^t \mathbf{X} = \mathbf{X}_{i,j} - \mathbf{X}_{i+1,j}$$

$$\mathbf{d}_{i,j,1}^t \mathbf{X} = \mathbf{X}_{i,j} - \mathbf{X}_{i+1,j+1}$$

$$\mathbf{d}_{i,j,2}^t \mathbf{X} = \mathbf{X}_{i,j} - \mathbf{X}_{i,j+1} \tag{17}$$

$$\mathbf{d}_{i,j,3}^t \mathbf{X} = \mathbf{X}_{i,j} - \mathbf{X}_{i-1,j+1}.$$

The second part of the assumption can be acted on by exploiting the correlation between the color channels to determine the true edges in the image. At locations where true edges have been determined, no smoothing is done to ensure the edges are maintained.

These criteria can be met by using the convex quadratic correlator function with a line process, defined as

$$\rho(a) = \begin{cases} 0, & \text{if an edge is detected} \\ a^2, & \text{otherwise} \end{cases}. \tag{18}$$

When a correlated edge is not detected, the quadratic term produces a least squares fit to the data, smoothing out the false edges. When an edge is detected, no cost is associated with this term, aligning and preserving the true
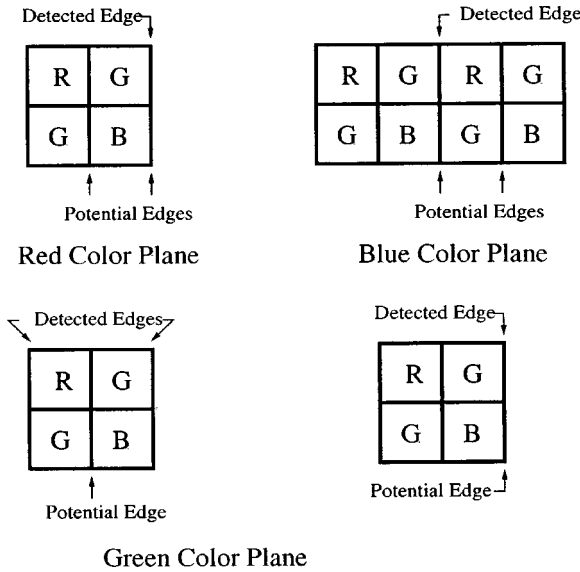
Red Color Plane

Blue Color Plane

Green Color Plane

Fig. 3 Detected and potential edges.

Fig. 4 Correlated edges.

edges. Note that the convexity of $\rho(\cdot)$ ensures that the minimization remains convex and the results stable.[16,17]

A strong correlation exists between the individual color planes of a full color image. An edge of an object is often present and aligned in more than one color plane. Images that have been subsampled using a single chip CCD array lose this correlation due to the physical separation of the individual elements in the array.

Let a detected edge be defined as a location where the directional derivative is greater than some threshold,

$$\mathbf{d}_{i,j,m}^{t}\mathbf{X} > T, \tag{19}$$

where T is the value of that threshold. Let a potential edge be defined as a location where a true edge may have been originally located based on the presence of a detected edge. The process of correlated edge detection is accomplished by first detecting the edges present in each of the color planes, determining the location of potential edges, and finally determining the actual edges by matching up the correlated potential edges.

Consider the problem of locating edges in the direction $\mathbf{d}_{i,j,0}^{t}\mathbf{X}$. Figure 3 illustrates how potential edge locations follow from the location of detected edges. The RGB cubes represent the 2×2 sampling blocks of the CCD array with the sampling for each of the primary colors indicated.

The location of potential edges follows naturally from the knowledge of the forward process and the location of the detected edges. If an edge is detected in the red or blue color planes, the actual edge could have been located at any point, since that particular color plane was last sampled. In the green color plane, identifying potential edges is a little more challenging. This is because the green value of a pixel is the average of two sample points. If an actual edge is located in the center of a 2×2 sampling block, the edge is smoothed and replaced by a two-step edge.

The final step of correlated edge detection is to reconstruct the actual edge information given the potential edges.
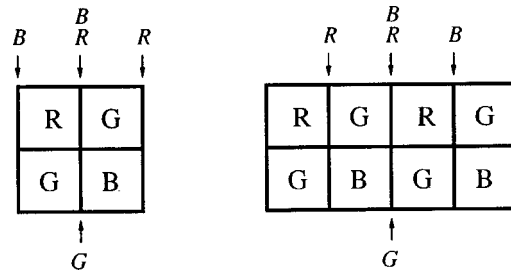
Figure 4 shows that potential edges from all the color planes line up at the location of the actual edge.

It is not always the case, however, that edges contain edge information in all color planes. It may be that an actual edge only exists in one color plane. Therefore, a method of determining actual edge location is needed, which is independent of the number of color planes that contain potential edges. To include these cases, the actual edge is said to exist at the location with the highest number of potential edges. In the case of a tie, the actual edge is said to exist at the location it was detected, (i, j).

The previous development describes a method for identifying correlated edges in the direction $\mathbf{d}_{i,j,0}^{t}\mathbf{X}$. The detection of edges in the other directions follows a similar development.

The necessary motivation now exists to introduce the functional form using a Markov random field model and the quadratic correlator function $\rho(\cdot)$. The proposed exponential kernel of the modified Gaussian Markov random field (GMRF) image model is

$$\Omega[\mathbf{X}] = \sum_{c \in C} V_c(\mathbf{X}) = \sum_i \sum_j \sum_{m=0}^{3} \rho(\mathbf{d}_{i,j,m}^{t}\mathbf{X}), \tag{20}$$

where $\Omega[\mathbf{X}]$ is a function of the fully specified image $\mathbf{X}$. To find the MAP estimate $\hat{\mathbf{X}}$, the convex functional $\Omega[\mathbf{X}]$ must be minimized subject to the constraint $\mathbf{X} \in \mathcal{Z}$.

A steepest descent projection technique was selected to minimize the functional in Eq. (20). This constrained optimization method performs a steepest descent step at each iteration.

Denote the image estimate at the n-th iteration as $\mathbf{X}^{(n)}$. The 0 iteration, $\mathbf{X}^{(0)}$, can be initialized using an expansion of the subsampled image data $\mathbf{Y}^*$ by replicating the sample values throughout the sampling neighborhood.

To update the image estimate $\mathbf{X}^{(n)}$ in each iteration, a step in a particular direction $\mathbf{v}^{(n)}$ is taken, where $\mathbf{v}^{(n)}$ is of the same size as $\mathbf{X}^{(n)}$. A common choice for this direction is the negative of the gradient direction, where the gradient direction can be found as,

$$\mathbf{u}^{(n)} = \left\{ \frac{\partial \Omega[\mathbf{X}^{(n)}]}{\partial \mathbf{X}^{(n)}} \right\}. \tag{21}$$
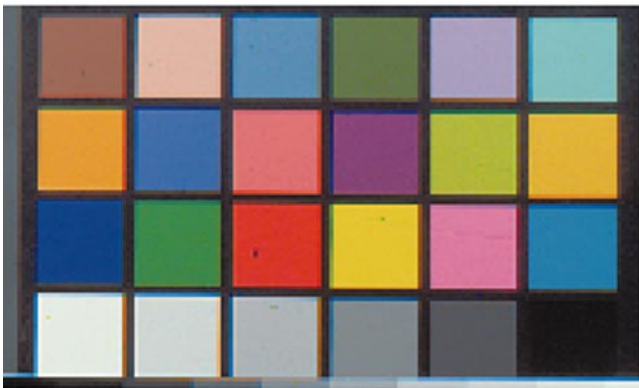
The direction of descent must then be mapped onto the constraint space to confine the update to the constraint of
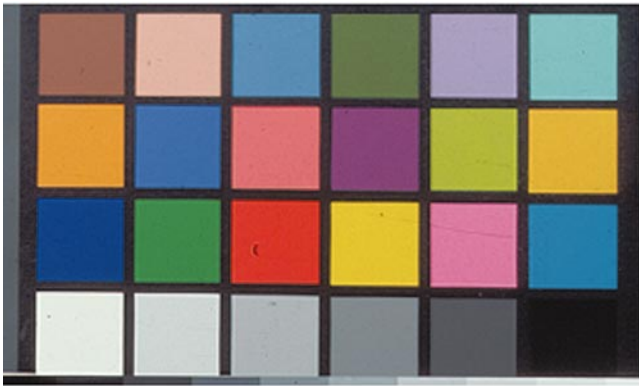
a) Original Image
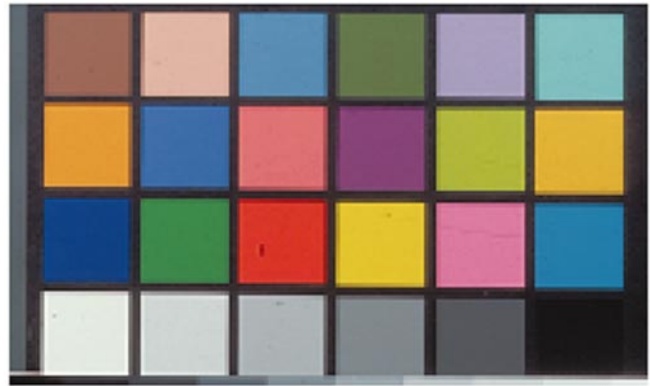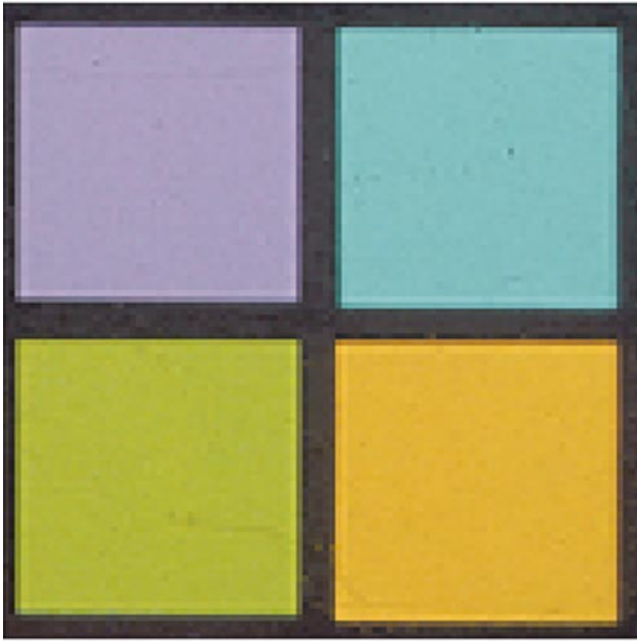
b) Properly Sub-Sampled Image
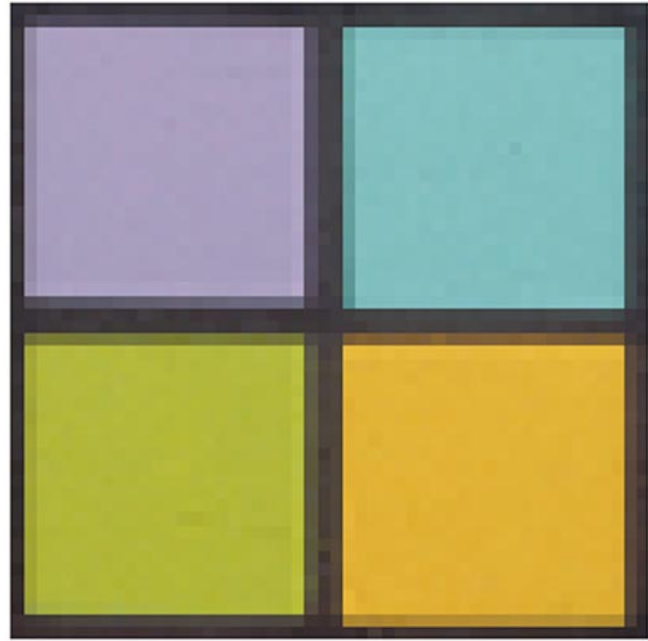
c) Improperly Sub-Sampled Image
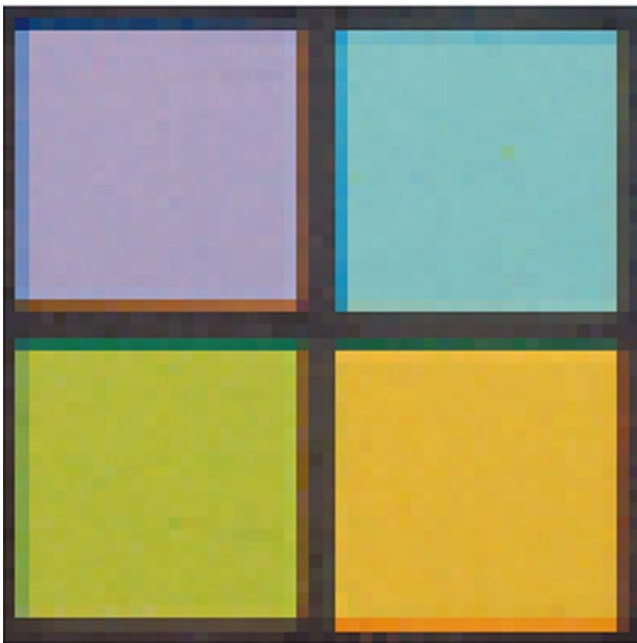
d) Image Enhanced
Using Proposed Algorithm

Fig. 5 Enhancement of color squares captured using single chip CCD arrays: (a) original image, (b) properly subsampled image, (c) improperly subsampled image, and (d) image enhanced using proposed algorithm.

a) Original Image

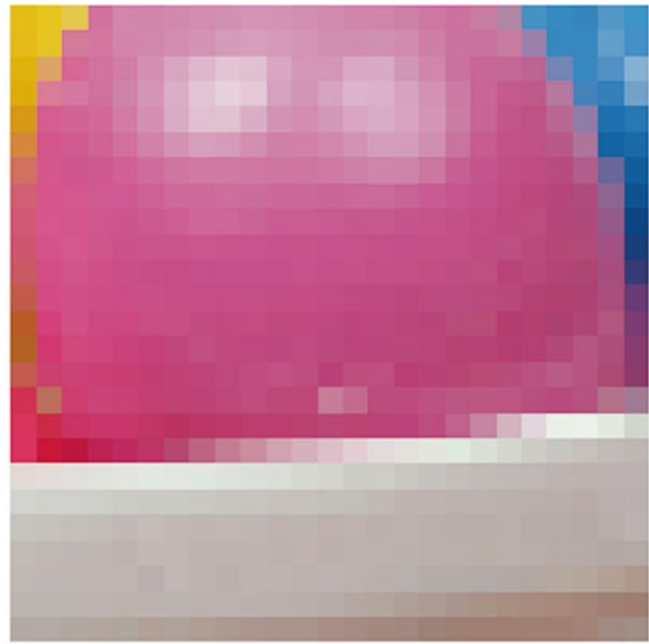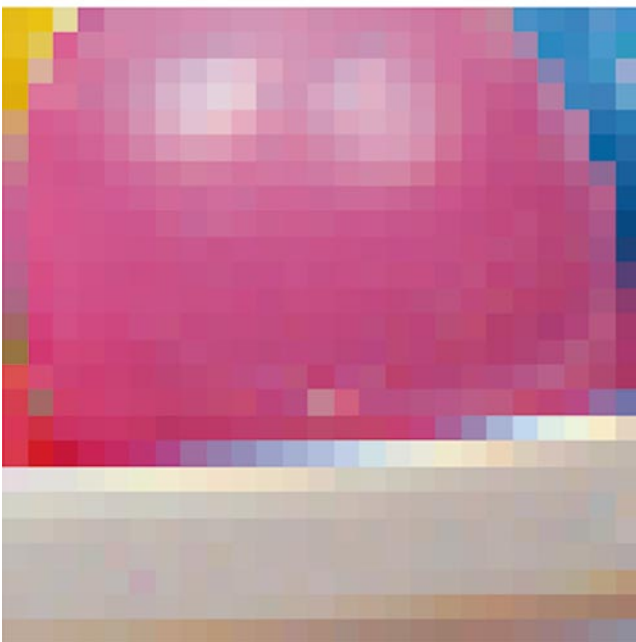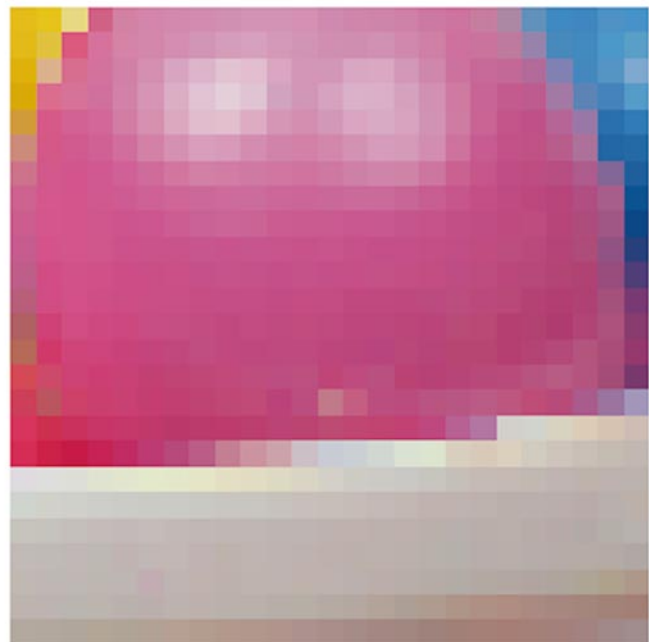b) Properly Sub-Sampled Image

c) Improperly Sub-Sampled Image

d) Image Enhanced
Using Proposed Algorithm

Fig. 6 Expansion of Fig. 5: (a) original image, (b) properly subsampled image, (c) improperly sub-sampled image, and (d) image enhanced using proposed algorithm.

a) Original Image

b) Properly Sub-Sampled Image

c) Improperly Sub-Sampled Image

d) Image Enhanced
Using Proposed Algorithm

Fig. 7 Enhancement of color eggs captured using single chip CCD arrays: (a) original image, (b) properly subsampled image, (c) improperly subsampled image, and (d) image enhanced using proposed algorithm.

a) Original Image

b) Properly Sub-Sampled Image

c) Improperly Sub-Sampled Image

d) Image Enhanced
Using Proposed Algorithm

Fig. 8 Expansion of Fig. 7: (a) original image, (b) properly subsampled image, (c) improperly sub-sampled image, and (d) image enhanced using proposed algorithm.

Eq. (14). Since the matrix defining the forward process is known, this projection matrix can be found as[18]

$$\mathbf{v}_{i,j} = -[I - \mathbf{S}^{*t}(\mathbf{S}^*\mathbf{S}^{*t})^{-1}\mathbf{S}^*]\mathbf{u}_{i,j}, \qquad (22)$$

$$
\mathbf{v}_{i,j} = -
\begin{bmatrix}
0 & 0 & 0 & 0 & 0 & 0 & 0 & 0 & 0 & 0 & 0 & 0 \\
0 & 1 & 0 & 0 & 0 & 0 & 0 & 0 & 0 & 0 & 0 & 0 \\
0 & 0 & 1 & 0 & 0 & 0 & 0 & 0 & 0 & 0 & 0 & 0 \\
0 & 0 & 0 & 1 & 0 & 0 & 0 & 0 & 0 & 0 & 0 & 0 \\
0 & 0 & 0 & 0 & 1 & 0 & 0 & 0 & 0 & 0 & 0 & 0 \\
0 & 0 & 0 & 0 & 0 & \frac{1}{2} & -\frac{1}{2} & 0 & 0 & 0 & 0 & 0 \\
0 & 0 & 0 & 0 & 0 & -\frac{1}{2} & \frac{1}{2} & 0 & 0 & 0 & 0 & 0 \\
0 & 0 & 0 & 0 & 0 & 0 & 0 & 1 & 0 & 0 & 0 & 0 \\
0 & 0 & 0 & 0 & 0 & 0 & 0 & 0 & 1 & 0 & 0 & 0 \\
0 & 0 & 0 & 0 & 0 & 0 & 0 & 0 & 0 & 1 & 0 & 0 \\
0 & 0 & 0 & 0 & 0 & 0 & 0 & 0 & 0 & 0 & 1 & 0 \\
0 & 0 & 0 & 0 & 0 & 0 & 0 & 0 & 0 & 0 & 0 & 0
\end{bmatrix}
\mathbf{u}_{i,j}.
$$

$$(23)$$

Now that the projection operator has been defined, the magnitude of the direction taken can be determined. Let

$$\mathbf{X}^{(n+1)} = \mathbf{X}^{(n)} + \alpha^{(n)}\mathbf{v}^{(n)}, \qquad (24)$$

where the scalar $\alpha^{(n)}$ represents the size of the step taken in the direction $\mathbf{v}^{(n)}$. For fast convergence, a value for $\alpha^{(n)}$ should be selected that gives the optimal step size toward the global minimum of the functional. This can be done by approximating the functional with a truncated Taylor series and selecting the step size that minimizes this approximation in the selected direction of descent.[19]

The process of determining descent direction, projecting onto the constraint space, and calculating the step size is repeated until the problem converges on a solution.

4 Experimental Results

This section demonstrates the value of the proposed algorithm through two representative examples. Figure 5 shows the results of subsampling and enhancing the image of an array of colored squares. Four images are shown: the original image, the properly and improperly subsampled images, and the enhanced image. In addition to the full size images, an expanded view of a single color block from each image is included to show greater detail (see Fig. 6). The original image was subsampled according to the processes of properly and improperly subsampling an image, discussed in Sec. 2. Notice the introduction of false colors along the edges in the improperly subsampled image. The enhanced image obtained from applying the algorithm proposed in this work shows an improvement in the quality of the edges. The artifacts such as the false colors due to uncorrelated edge information have been greatly reduced.

The example given in Fig. 7 shows the results of subsampling and enhancing the image of a bowl of colored eggs. Again four images are shown. An expanded view of the center of the image is shown in Fig. 8. Notice the introduction of false colors particularly along the top and bottom edges of the bowl. Also, false colors are present

Table 1 Signal to noise ratio of the interpolated images as compared to the original image.

Image	Colors	Eggs
Improperly subsampled	18.3 dB	18.3 dB
Enhanced	19.6 dB	19.2 dB

along the boundaries of the blue eggs in the subsampled image. These artifacts have been greatly reduced in the enhanced image.

Table 1 quantifies the experimental results. The SNR of the improperly subsampled image is compared to that of the results achieved using the proposed enhancement algorithm. In the case of both test images, a gain of approximately 1 dB is achieved.

5 Conclusion

The physical separation of the individual elements in a single chip CCD array cause the edges in the RGB color planes to become misaligned. This introduces artifacts such as false coloring along the edges of an image. Enhancing subsampled color image data is a useful step in producing a better quality image for viewing. We propose an enhancement algorithm based on stochastic regularization using a Gaussian image model with a deterministic line process to realign and maintain the edge information. The resulting computational algorithm involves an iterative constrained gradient descent, which requires a correlation operator to realign the edge information. Results show that the algorithm works well to reduce, and often eliminate, the visible effects of this type of image capture.

References

1. B. E. Schmitz and R. L. Stevenson, "The enhancement of color image data captured using single chip CCD arrays," *Proc. Conf. Image and Video Process. IV*, R. L. Stevenson and M. I. Sezan, Eds., *Proc. SPIE* **2666**, 97–106 (1996).
2. N. Ozawa and K. Takahashi, "A correlative coefficient multiplying (CCM) method for chrominance moire reduction in single-chip color video cameras," *IEEE Trans. Electron Devices* **38**(5), 1217–1225 (1991).
3. N. Ozawa, "Chrominance moire reduction using CCM signal interpolation single-chip color video camera," *ITEJ* **46**(2), 210–216 (1992).
4. H. Sugiura, K. Asakawa, and J. Fujino, "False color signal reduction method for single-chip color video cameras," *IEEE Trans. Consumer Electron.* **40**(2), 100–106 (1994).
5. S. Omori and K. Ueda, "High-resolution image using several sampling-phase shifted images," *Proc. IEEE Int. Conf. Consumer Electron.*, pp. 178–179 (June 2000).
6. D. S. Messing and M. I. Sezan, "Improved mult-image resolution enhancement for colour images captured by single-CCD cameras," *Proc. IEEE Int. Conf. Image Process.*, pp. 484–487 (Sep. 2000).
7. J. Go, K. Sohn, and C. Lee, "Interpolation using neural networks for digital still cameras," *IEEE Trans. Consumer Electron.* **46**(3), 610–616 (2000).
8. T. Sakamoto, C. Nakanishi, and T. Hase, "Software pixel interpolation for digital still cameras suitable for a 32-bit MCU," *IEEE Trans. Consumer Electron.* **44**(4), 1342–1352 (1998).
9. T. Toi, "Color signal processing technique for single-chip CCD cameras that employ CPUs with SIMD instruction sets," *IEEE Trans. Consumer Electron.* **46**(2), 291–294 (2000).
10. B. S. Hur and M. G. Kang, "High definition color interpolation scheme for progressive scan CCD image sensor," *IEEE Trans. Consumer Electron.* **47**(1), 179–186 (2001).
11. R. Kimmel, "Demosaicing: Image reconstruction from color CCD samples," *IEEE Trans. Image Process.* **8**(9), 1221–1228 (1999).
12. T. Kuno and H. Sugiura, "New interpolation method using discriminated color correlation for digital still cameras," *IEEE Trans. Consumer Electron.* **45**(1), 259–267 (1999).
13. R. W. G. Hunt, *The Reproduction of Colour in Photography, Printing*

。